

IR Detection of H₂O₂ at 80 K in Ion-Irradiated Laboratory Ices Relevant to Europa

M. H. Moore

Code 691, Astrochemistry Branch, NASA/Goddard Space Flight Center, Greenbelt, Maryland 20771
E-mail: ummhm@lepvax.gsfc.nasa.gov

and

R. L. Hudson

Department of Chemistry, Eckerd College, St. Petersburg, Florida 33733

Received June 7, 1999; revised November 17, 1999

We present the first *in situ* laboratory detection of H₂O₂ in H⁺ irradiated ices at temperatures relevant to the icy Galilean satellites. These experiments were motivated by the recent Galileo NIMS detection on Europa of a 3.5-μm band identified with H₂O₂ (R. W. Carlson *et al.* 1999, *Science* 283, 2062–2064). In our laboratory experiments, the IR signature of H₂O₂ was easily observed after irradiation of pure H₂O at 16 K, but it was not seen after irradiation at 80 K. Radiolysis of mixtures of H₂O with O₂ or CO₂ at 80 K did produce H₂O₂. These results show that ices more complex than pure H₂O are involved in the radiolysis pathway to form H₂O₂ on Europa. We also report the intrinsic band strength and radiation yield of H₂O₂ in ice mixtures, along with possible formation and destruction mechanisms. Sufficient concentrations of H₂O₂ can be formed in H₂O ices containing O₂ to explain the NIMS observation.

© 2000 Academic Press

Key Words: radiation chemistry; ices; Europa; infrared observations; satellites of Jupiter.

INTRODUCTION

Hydrogen peroxide has been identified on Europa based on a 3.50-μm absorption feature in Galileo NIMS spectra, along with corroborating evidence from profiles at shorter wavelengths in Galileo UVS spectra (Carlson *et al.* 1999). The position and width of the IR feature were matched with a laboratory reflectance spectrum of H₂O + H₂O₂ ice; the intensity of the NIMS feature suggested an H₂O₂ concentration of 0.13% by number relative to H₂O. Europa has a constant flux of energetic ions bombarding its surface, therefore H₂O₂ is thought to be a radiation product. Based on the reported radiation yield for H₂O₂ in H₂O ice, Carlson *et al.* (1999) concluded that the surface abundance of H₂O₂ on Europa, after factoring in production and loss rates thought to be relevant, would be 0.013 to 0.3% relative to H₂O, a number consistent with the observations.

Table I summarizes the known condensed-phase molecules on Europa, Ganymede, and Callisto. These satellites of Jupiter have H₂O ice on their surfaces. Condensed-phase molecular oxygen has been detected on Ganymede along with O₃; on Europa a tenuous oxygen atmosphere has been observed (Hall *et al.* 1998). All of these icy satellites exist in the radiation environment of Jupiter, and the intensities and energies of particles (H⁺, Oⁿ⁺, Sⁿ⁺, and e⁻) bombarding their surfaces varies with, e.g., the distance of the satellite from Jupiter, and the satellite's intrinsic magnetic field and atmospheric density. The estimated value of the incident energy flux (Cooper *et al.* 2000) is included in Table I for each satellite. Although Europa receives the highest flux of energetic particles, the other satellites receive enough radiation that the formation of products like H₂O₂ seems likely.

The influence of ionizing radiation on frozen water has been studied for many years with most early work focusing on the identities and yields of stable products, namely H₂, O₂, and H₂O₂. In a typical experiment, an ice was irradiated and subsequently melted for analysis. Since transient, highly reactive species like trapped electrons, OH, H, and HO₂, cannot be detected this way, they have been studied at low temperatures with *in situ* methods such as UV-visible spectroscopy or electron spin resonance spectroscopy. Pulse radiolysis also has been employed for detection of transients in irradiated ice.

Traditionally the yield of a radiation product has been denoted by a *G* value, defined as the number of molecules of a certain type formed per 100 eV of energy absorbed. Numerous workers have studied H₂O₂ production in ice and reported on how *G*(H₂O₂) and the final H₂O₂ abundance are influenced by temperature, the initial composition of the ice, and the type of radiation used. For example, Ghormley and Stewart (1956) measured H₂O₂ production in ice γ -irradiated at several temperatures, and found that the final abundance of H₂O₂ was lowest at their highest irradiation temperatures. However, they also found

TABLE I
Icy Galilean Satellites

Satellite	Condensed phase molecules identified	Temperature range	Total average energy flux, $E > 20 \text{ keV}^a$ (eV cm ⁻² s ⁻¹)
Europa	H ₂ O, CO ₂ ^b , SO ₂ ^c , H ₂ O ₂ ^d	85–128 K ^{e,f}	78×10^{12}
Ganymede	H ₂ O, CO ₂ ^g , SO ₂ ^h , O ₂ ⁱ , O ₃ ^j	85–152 K ^{e,f}	5.4×10^{12} poles 0.3×10^{12} equator
Callisto	H ₂ O, CO ₂ ^g , SO ₂ ^{h,k} , O ₃ ^l	80–150 K ^f	0.2×10^{12}

^a Cooper *et al.* (2000), lower limit of energetic ions and electron flux based on EPD experiment on Galileo Orbiter.

^b Smythe *et al.* (1998).

^c Lane *et al.* (1981), Noll *et al.* (1995).

^d Carlson *et al.* (1999).

^e Orton *et al.* (1996).

^f Hanel *et al.* (1979).

^g Carlson *et al.* (1996), McCord *et al.* (1997), McCord *et al.* (1998).

^h McCord *et al.* (1997), McCord *et al.* (1998).

ⁱ Spencer *et al.* (1995).

^j Noll *et al.* (1996).

^k Noll *et al.* (1997).

^l Associated with impact area.

that at the higher irradiation temperatures the amount of H₂O₂ formed could be increased by adding O₂ to the ice before freezing and irradiating. In all cases the irradiated ices had to be melted for H₂O₂ analysis; no *in situ* H₂O₂ determinations were possible.

Although γ - and X-ray experiments provide insight into the radiation chemistry of ice, ion irradiations are more relevant to icy satellites. Unfortunately, *in situ* measurements of $G(\text{H}_2\text{O}_2)$ are also lacking for ion irradiations. The Galileo NIMS data was interpreted (Carlson *et al.* 1999) with $G(\text{H}_2\text{O}_2) = 0.4$ for α irradiation of ice; however, the source of this value is surprisingly elusive. We have traced this $G(\text{H}_2\text{O}_2)$ to Lefort (1955), a paper which gives few analytical details of the H₂O₂ analysis. However, earlier papers (Bonet-Maury and Lefort 1948, Bonet-Maury and Frilley 1944, Bonet-Maury 1941, 1944) make it clear that the irradiated ices were melted prior to measurement of $G(\text{H}_2\text{O}_2)$ near room temperature with a colorimetric method.

In this paper we present laboratory results for proton-irradiated ices, along with *in situ* measurements of H₂O₂ production. By studying these ices in the solid state, we are able to avoid the uncertainties introduced by melting samples for H₂O₂ analysis. The temperatures chosen for our irradiations and H₂O₂ analyses were 16 and 80 K, the latter being more relevant for jovian satellites. Although H₂O₂ was easily observed after irradiation of pure H₂O ice at 16 K, contrary to our expectations it was not seen after irradiation at 80 K. If, however, the 80 K H₂O ice contained either O₂ or CO₂, then H₂O₂ was detected after irradiation. Overall, the band position and width of the H₂O₂ feature showed some variation with composition,

concentration, and temperature. We also have measured the intrinsic IR band strength, the A value, of the H₂O₂ band near 3.5 μm , the same band used to identify H₂O₂ in the NIMS data. The H₂O₂ band strength and our IR spectra after irradiation have been combined to give H₂O₂ yields for different ice mixtures.

EXPERIMENTAL

Ice films a few microns in thickness were formed in two different ways on an aluminum mirror attached to the tail section of a closed-cycle cryostat. First, for each irradiation experiment an ice film was formed by gas-phase condensation at 16 K, and the resulting ice thickness was determined by measuring interference fringes during deposition. Second, ices of H₂O + H₂O₂ were made by using a syringe to inject a solution through a vacuum septum onto the precooled mirror (~ 16 K). In both cases, the ice temperature could be maintained between ~ 16 and 300 K. The results reported in this paper do not depend on the precise value of the minimum temperature.

Infrared absorption spectra of all ices were measured by passing an IR beam through the ice film, reflecting it from the ice-aluminum interface, and again passing it through the ice. However, analysis of spectra to calculate column density was based on the physical thickness of the ice, not the IR thickness. The resolution of the spectrometer for these experiments was 4 cm^{-1} . Reported spectral positions are accurate to $\pm 0.5 \text{ cm}^{-1}$.

Protons (0.8 MeV) from a Van de Graaff accelerator were used to irradiate ices at 16 and 80 K. A nickel beam foil separated the vacuum of the accelerator from the clean vacuum of the cryostat area. Details of this experimental setup are already in print (Moore *et al.* 1996, Hudson and Moore 1995, and references therein).

Quantitative analysis of IR spectra of irradiated ices involved two steps. First, $A(\text{H}_2\text{O}_2)$ for the 3.5- μm band had to be measured. The injection technique was used to form different thicknesses of H₂O + H₂O₂ ice at ~ 16 K. The area of the H₂O₂ (3.5 μm) band was plotted against the area of the H₂O band at 753 cm^{-1} (13.3 μm) for each ice thickness. The slope of a line connecting these data is proportional to $A(\text{H}_2\text{O}_2)/A(\text{H}_2\text{O})$, the value of $A(\text{H}_2\text{O})$ being known at ~ 16 K from Hudgins *et al.* (1993). Our data gave $A(\text{H}_2\text{O}_2) = 2.7 \times 10^{-17} \text{ cm molecule}^{-1}$ at ~ 16 K. Next, the H₂O₂ band in each irradiated ice was integrated for every proton dose. Dividing the integrated band's areas by $A(\text{H}_2\text{O}_2)$ gave the column density of H₂O₂ in each ice as a function of radiation dose. To compare our results with estimates of the %H₂O₂ on Europa, column densities of H₂O₂ were converted to %H₂O₂ by number relative to H₂O.

The sources and purities of the reagents used in these experiments are as follows: triply distilled H₂O with a resistance greater than 10^7 ohm cm ; H₂O₂ (J. T. Baker), 30%; H₂O₂, standard pharmaceutical reagent, 3%; O₂ (Matheson), 99.6%; ¹⁸O₂ (Alfa), 99% ¹⁸O; CO₂ (Matheson), 99.995%; C¹⁸O₂ (Isomet), 95% ¹⁸O; N₂O (Airco), 99%.

RESULTS

(a) IR Spectrum of $H_2O + H_2O_2$

Figure 1 shows the IR spectrum of $H_2O + H_2O_2$ at 16 K from 3.2–4.0 μm . The H_2O_2 concentration was determined by $KMnO_4$ titration, before injection, to be 2.66% by mass or 1.4% by number relative to H_2O . The band at 2855 cm^{-1} (3.503 μm) in Fig. 1, with a full width at half maximum (FWHM) of 74 cm^{-1} (0.09 μm), was identified with the $\nu_2 + \nu_6$ combination mode (also possibly $2\nu_6$ and $2\nu_2$) of H_2O_2 (Lannon *et al.* 1971, Pettersson *et al.* 1997). The underlying, sloping continuum on which the H_2O_2 feature sits in Fig. 1 is part of the 3260 cm^{-1} (3.07 μm) water band. This same H_2O_2 absorption was measured at 80 K by diffuse reflection (Carlson *et al.* 1999), after cooling a liquid H_2O_2 solution from room temperature, and found to be at 2854 cm^{-1} (3.504 μm) with a FWHM of $\sim 49 \text{ cm}^{-1}$ ($\sim 0.06 \mu\text{m}$). We warmed a 1.4% H_2O_2 ice from 16 to 160 K and found that the band position changed from 2855 cm^{-1} (3.503 μm) to 2845 cm^{-1} (3.515 μm) and the FWHM decreased as the sample became crystalline. Similar behavior was observed on warming a more concentrated sample, 14% H_2O_2 , to 160 K.

(b) Irradiated Pure H_2O

A 3- μm -thick film of H_2O was irradiated at $\sim 16 \text{ K}$ to a total dose of $17 \text{ eV molecule}^{-1}$. After irradiation H_2O_2 was detected on the wing of the H_2O band, with a peak position at 2856 cm^{-1} (3.501 μm) and a FWHM of 49 cm^{-1} (0.06 μm). The position and width of this H_2O_2 band were essentially unchanged from ~ 16 to 120 K. The experiment was then repeated at 80 K, but to our surprise no H_2O_2 was detected after irradiation. This result led us to examine the radiolysis of icy mixtures relevant to Europa which might form H_2O_2 .

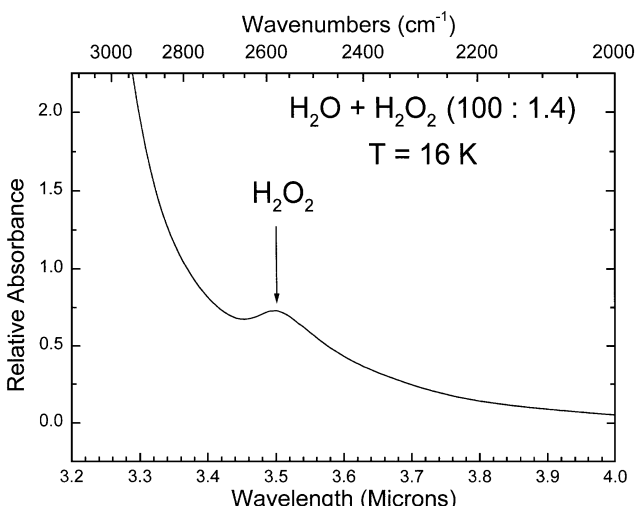


FIG. 1. IR spectrum of $H_2O + H_2O_2$ (100 : 1.4) ice at 16 K between 3.2 and 4.0 μm . The 3.508- μm absorption feature due to H_2O_2 is on a sloping continuum due to the long wavelength wing of the 3- μm H_2O band.

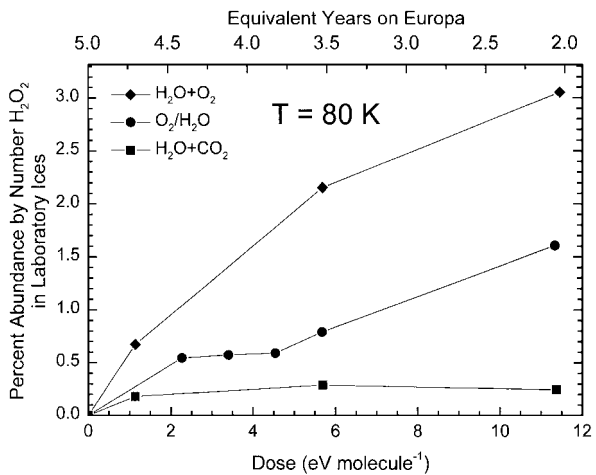


FIG. 2. The change in percentage abundance by number of H_2O_2 as a function of proton dose is plotted for three different ice mixtures: $H_2O + O_2$, O_2/H_2O , and $H_2O + CO_2$. The slope of each data set is the yield, $G(H_2O_2)$, for that mixture irradiated at 80 K.

(c) Irradiated $H_2O + O_2$

To investigate the influence of the addition of O_2 to H_2O on the formation of H_2O_2 , we condensed a gaseous mixture of $H_2O + O_2$ (8 : 1) at $\sim 16 \text{ K}$. The ice was slowly warmed to 80 K and then irradiated. This 8 : 1 mixture gave a very clear H_2O_2 feature at 2841 cm^{-1} (3.520 μm) with a FWHM of 121 cm^{-1} (0.15 μm). Figure 2 shows the change in the abundance of H_2O_2 in this irradiated ice as a function of deposited energy.

Although pure O_2 vaporizes in our 10^{-7} torr vacuum near 30 K, we expected that some O_2 would be trapped in the bulk ice (Ghormley 1967) during warming to 80 K. One indication of the presence of trapped O_2 was the IR detection of the ν_3 mode of O_3 at 1034 cm^{-1} (Brewer and Wang 1972) after irradiating the 80 K $H_2O + O_2$ ice. We estimate that $\sim 60\%$ of the O_2 is retained in the H_2O ice during warming, which results in an $H_2O + O_2$ ($\sim 100 : 8$) at 80 K. This result is based on a comparison of the areas of the O_3 band formed for similar radiation doses on $H_2O + O_2$ (8 : 1) ices at 18 K and that same original ice composition warmed and irradiated at 80 K. The estimate assumes that the yield of $O_2 \rightarrow O_3$ is the same at both temperatures.

(d) Irradiated O_2 on Top of H_2O (O_2/H_2O)

In another experiment, H_2O_2 formed in H_2O ice irradiated at 80 K when some O_2 was present at or near the surface of the ice. This condition was created by first forming a few-micrometers-thick layer of H_2O ice at $\sim 16 \text{ K}$ and then adding an equal thickness of O_2 ice on top of it (notation for this layered experiment is: O_2/H_2O). This layered ice was slowly warmed to 80 K before irradiation. Although most of the O_2 vaporized during warming, some fraction was bound to the water surface or was trapped in the top portion of the porous amorphous water ice (Ghormley 1967). After irradiation, H_2O_2 was detected in the infrared spectrum at 2851 cm^{-1} (3.508 μm) with a FWHM of

83 cm⁻¹ (0.10 μm). A factor of 2–3 less H₂O₂ was formed in this experiment compared with the experiment where O₂ was more intimately mixed and trapped in the bulk ice. Results from this O₂/H₂O experiment are also plotted in Figure 2. The smaller amount of trapped O₂ probably explains why O₃ was not detected in this experiment. Without the formation of detectable O₃ we were unable to estimate the amount of O₂ trapped on the surface at 80 K.

(e) H₂O + CO₂

Since CO₂ has also been identified on the surface of Europa (Table I), we studied irradiated H₂O + CO₂ (8 : 1) ice to examine other possible formation pathways for H₂O₂. Irradiated H₂O containing CO₂ formed H₂O₂ with a broad band at 2851 cm⁻¹ (3.508 μm) and a FWHM of 101 cm⁻¹ (0.12 μm). Figure 2 shows the change in percentage abundance of H₂O₂ in the irradiated ice at 80 K as a function of radiation dose.

(f) Other Ice Mixtures

A few supporting experiments were done at ~16 and 80 K with isotopically labeled molecules. A 10 : 1 mixture of H₂O + C¹⁸O₂ was irradiated, and H₂O₂ was seen at the same position as in the H₂O + C¹⁶O₂ mixture. An 8 : 1 H₂O + ¹⁸O₂ mixture was irradiated, and the peak position of H₂O₂ occurred 10 wave-numbers less than in the H₂O + ¹⁶O₂ experiment.

Many other experiments were performed to determine if H₂O₂ formation was common in irradiated ice mixtures. Ices made of H₂O and other molecules, containing carbon, hydrogen, nitrogen, and oxygen, did not produce H₂O₂ during irradiation with one exception. When a 10 : 1 mixture of H₂O + N₂O (nitrous oxide) was irradiated, at either 16 or 80 K, the 3.50-μm band of H₂O₂ band was easily observed. The significance of this experiment will be discussed below. We hope to extend our work to sulfur-containing molecules in the near future.

DISCUSSION

(a) Comparison of Laboratory Spectra with the Europa Spectrum

In our experiments, the 3.5-μm H₂O₂ band's position and width were influenced by several factors. First, the position of the band changed with ice composition. In O₂/H₂O and H₂O + CO₂ irradiated ices at 80 K the peak positions were within the limits of the observed H₂O₂ feature on Europa, 3.50 ± 0.015 μm. However, the location of the H₂O₂ band in our H₂O + O₂ experiment was outside the limits of the Europa observation by +0.005 μm. Second, we found that the position of H₂O₂ in H₂O mixtures depended on the H₂O₂ concentration. In a 1.4% H₂O₂ solution frozen at ~16 K the peak was at 2855 cm⁻¹ (3.503 μm), but at 2843 cm⁻¹ (3.517 μm) for a similarly frozen 14% solution. The FWHM of the 3.5-μm band in these icy mixtures varied from 74 to 96 cm⁻¹ (0.09–0.12 μm, respectively). The width of the H₂O₂ band in the Europa observation, and the H₂O₂ 80 K

reference spectrum measured by Carlson *et al.* (1999) in diffuse reflection, was ~49 cm⁻¹ (0.06 μm). Finally, we observed that the FWHM of the H₂O₂ band in both the 1.4% and the 14% H₂O₂ ice decreases ~40% from 18 K (a temperature where the phase of H₂O ice is amorphous) to 160 K (a temperature where the phase of H₂O ice is crystalline). Table II summarizes the peak position and FWHM of the 3.5-μm H₂O₂ band observed for different conditions.

Carlson *et al.* (1999) concluded that their laboratory measurements indicated a surface concentration of H₂O₂ on Europa near 0.13%, by number relative to water ice. This concentration is at the limit of detectability for transmission IR spectra of synthesized H₂O₂ in laboratory ices, which we estimated to be at the 0.1–0.2% level. Variations in the peak position and width depend on the composition and H₂O₂ concentration of the ice along with other factors such as grain size, porosity, and thermal history. Detectability of weak features may also be affected by the difference between diffuse reflection measurements of bulk ice compared to absorption in a thin film. The identification and suggested concentration of H₂O₂ on Europa given by Carlson *et al.* (1999) is consistent with our laboratory experiments. It is the nature of the ices that leads to the H₂O₂ formation that is more complex than previously thought.

(b) Yield of H₂O₂

We have calculated *in situ* yields of H₂O₂ for the experiments done at 80 K. These yields are more relevant for icy satellites than those from previous studies on H₂O₂, where *G*(H₂O₂) was measured after the irradiated ice had been melted. Our *G* values are calculated during the early part of experiments when the production of H₂O₂ increases linearly with dose. The slopes for the curves in Fig. 2 give *G*(H₂O₂) for each ice studied. We used all of the data points for H₂O + O₂ and O₂/H₂O and the first data point for H₂O + CO₂ ice to determine the slopes. *G*s determined at higher doses in these experiments are less useful because product saturation occurs. The average *G*(H₂O₂) for the H₂O + O₂ experiment was 0.41, for O₂/H₂O it was 0.16, and for H₂O + CO₂ it was 0.10. For comparison, *G*(H₂O₂) = 0.1 in pure H₂O at ~16 K.

From the range of our *G*(H₂O₂)s, 0.1 to 0.4, the estimated steady-state percentage abundance of H₂O₂ on Europa is 0.07–0.28% assuming a lifetime of 100 days and an energy flux of 50×10^{12} eV cm⁻² s⁻¹ as discussed by Carlson *et al.* (1999). The *G*(H₂O₂) = 0.4 they used, which was based on analyses of ices melted after irradiation, was the largest *G*(H₂O₂) we measured *in situ* for our H₂O + O₂ irradiated ice. Using the above assumptions about Europa's environment, both H₂O + O₂ and O₂/H₂O mixtures on Europa could form a detectable steady-state concentration of H₂O₂; a mixture of H₂O + CO₂ would not, for an assumed lifetime of 100 days. Obviously the proper choice of *G* requires knowledge of the composition of the ice on Europa. If H₂O + CO₂ is an important contributor to the H₂O₂ concentration, adjustments to the model will be required. For example, the steady-state abundance increases by decreasing

TABLE II
Observed Band Position for H₂O₂ in the 3.5-μm Region

Observation of H ₂ O ₂	Conditions	H ₂ O ₂ peak position in the 3.5-μm region		FWHM (μm)
		cm ⁻¹	μm	
Europa spectrum ^a		2857 ± 12	3.50 ± 0.015	~0.06
Laboratory results				
H ₂ O + H ₂ O ₂ (100 : 13) ^a	Diffuse reflection IR, 300 K liquid cooled to 80 K	2854	3.504	~0.06
H ₂ O, UV photolysis ^b	Transmission IR, 10 K Warmed to 70 K	2860 ^c 2860 ^c	3.496 3.496	0.08 0.08
Laboratory results, this paper	Transmission IR			
H ₂ O + O ₂ , p ⁺ irr.	T = 80 K	2841	3.50	0.15
O ₂ /H ₂ O, p ⁺ irr.	T = 80 K	2851	3.508	0.10
H ₂ O + CO ₂ , p ⁺ irr.	T = 80 K	2851	3.508	0.12
H ₂ O, p ⁺ irr.	T = 18 K	2856	3.501	0.06
	Warmed to 120 K	2855	3.500	0.05
H ₂ O + H ₂ O ₂ (100 : 1.4)	T = 18 K	2855	3.503	0.09
	Warmed to 80 K	2854	3.504	0.08
	Warmed to 160 K	2845	3.515	0.05
H ₂ O + H ₂ O ₂ (100 : 14)	T = 18 K	2843	3.517	0.12
	Warmed to 80 K	2841	3.520	0.11
	Warmed to 160 K	2842	3.519	0.07

^a Carlson *et al.* (1999).

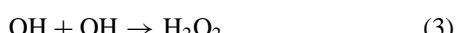
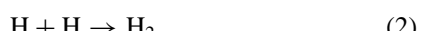
^b Gerakines *et al.* (1996).

^c Gerakines (pers. commun.).

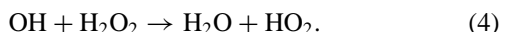
the destruction rate, or by assuming smaller ice densities (our calculations and those of Carlson *et al.* (1999) are based on an ice density of 1 g cm⁻³). Alternatively, a model in which more H₂O₂ is concentrated in the top few tens of micrometers of the ice, instead of averaged over the range of the most penetrating particle (180 μm for electrons), would increase the percentage abundance detected. The proper value of G also needs to include any contributions from electrons and heavy ions whose energy fluxes are about the same as for protons.

(c) Formation Mechanisms for H₂O₂

In our experiments, the initial radiation effect is the creation of ionization and excitation events in an ice along the tracks of the incident protons. Ionization of molecules will produce electrons which may either enter into chemical reactions or, given sufficient energy, form a separate track of radiation events. In H₂O, both H and OH radicals are formed during radiolysis and can undergo radical–radical reactions to reform H₂O and to make H₂ and H₂O₂:



The density of radicals formed in an individual event increases with the stopping power of the ion. Since radical–radical reactions are more important as the stopping power of the incident radiation rises, we expect our yield of H₂O₂ to be greater than in γ- and X-ray experiments, but perhaps lower than in α irradiations. Since HO₂ is reported (Swallow 1973) to be one of the primary products in ion irradiated ices, then we expect HO₂ to be formed in our proton irradiated ices due to the high stopping power of the proton. The reaction normally invoked to explain HO₂ formation involves the destruction of peroxide:



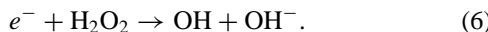
The most striking result in our work is probably the lack of H₂O₂ at 80 K in irradiated H₂O ice. Most likely, peroxide is made at 80 K, but its concentration is below our IR detection limit, which is about 0.1 mol%. It is difficult to decide upon one single mechanism to explain why H₂O₂ is seen in our irradiated amorphous H₂O ices at 16 K but not at 80 K. One possibility is that reaction (4) may be more efficient at removing H₂O₂ at 80 K than at 16 K. A second possibility is that hydrogen molecules may play a role in limiting reaction (4) at 16 K by reacting with

OH radicals:



In other words, reactions (4) and (5) may compete for “free” OH radicals. Because H₂ is removed by sublimation at 80 K, then more OH will be available for reaction (4) at 80 K than at 16 K, lowering the observed H₂O₂ abundance.¹ A third possibility is that reaction (1), reformation of H₂O, is more efficient at 80 K than at 16 K, lowering the H₂O₂ yield at the higher temperature. Evidence for an enhancement of reaction (1) near 80 K relative to 16 K is provided by experiments on the radiation amorphization of crystalline H₂O ice (Moore and Hudson 1992). Ice at 77 K shows a much greater resistance to amorphization than at 16 K, apparently due to the higher efficiency of the H + OH reaction. In the absence of additional data, it is difficult to decide which, if any, of these mechanisms is the most important. Reactions (1)–(5) may well be simplifications of processes involving solid-state defects in ices, but these reactions are thought to reflect the proper stoichiometry.

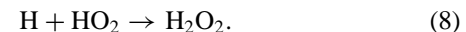
As an alternative to the above mechanisms, we also have considered the reaction of H₂O₂ with electrons produced by the incident radiation:



At room temperature, destruction of H₂O₂ by this reaction is orders of magnitude faster than either reaction (4) or reaction (5). Since electron trapping in ice is expected to be smaller at 80 K than 16 K, more e^- will be available at the higher temperature for reaction with H₂O₂ by reaction (6). This is consistent with the absence of H₂O₂ from the spectra of H₂O ice irradiated at 80 K. Reaction (6)’s importance in our ices was examined in two separate experiments at 80 K involving efficient electron “scavengers,” namely CO₂ and N₂O. Although pure H₂O ice irradiated at 80 K did not show H₂O₂, when either an H₂O + CO₂ or H₂O + N₂O ice was irradiated at 80 K, H₂O₂ was clearly seen. Our interpretation is that in the later two cases, CO₂ and N₂O consumed some of the available electrons, preventing them from destroying H₂O₂ by reaction (6). The result was a greater yield of H₂O₂, which was reflected in the increase in the H₂O₂ band strength. These experiments demonstrate that an electron scavenger can influence H₂O₂ abundances in irradiated ices and may explain changes in H₂O₂ abundances with temperature.

The formation of H₂O₂ in H₂O ice having O₂ either mixed in or adsorbed on its surface is perhaps easier to understand. We have previously shown that H-atom addition reactions result during proton irradiation of H₂O + C₂H₂, forming C₂H₄ and C₂H₆ (Moore and Hudson 1998), and during irradiation of H₂O + CO, forming H₂CO and CH₃OH (Hudson and Moore 1999). H-atom addition to O₂ to form H₂O₂ should proceed with little difficulty. Radiolysis generates H atoms from H₂O which may then add

sequentially to O₂ to make peroxide:

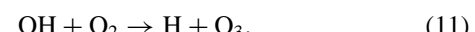


Our experiment with H₂O + ¹⁸O₂ is consistent with these reactions since it showed that H₂¹⁸O₂ was formed (see Results, Section f). This identification was supported by numerous experiments which compared the position of H₂O₂ in irradiated H₂¹⁶O, H₂¹⁸O, H₂¹⁶O + ¹⁶O₂, and H₂¹⁸O + ¹⁸O₂ ices. An alternative to reaction (7) is that O₂ may capture electrons to form O₂⁻ which is then protonated to make HO₂, followed by reaction (8) to peroxide.

We also have observed O₃ formation in experiments on ice samples made from O₂ and H₂O. The simplest ways that O₃ can be made are probably O-atom addition,



or O-atom transfer from a hydroxyl radical,



Our experiment with a H₂¹⁶O + ¹⁸O₂ mixture confirmed that both ¹⁸O₃ and ¹⁶O¹⁸O₂ are formed, as predicted by reactions (9)–(11). These results concerning O₃ will be presented in a future paper.

Finally, peroxide was observed at both 16 and 80 K in our radiation experiments with H₂O + CO₂ ice. It is likely that CO₂ scavenges electrons, protecting H₂O₂ from destruction at 80 K by reaction (6). This agrees with our H₂O + C¹⁸O₂ experiment: the H₂O₂ synthesized was at the same IR position as H₂O₂ made from the H₂O + C¹⁶O₂ mixture. Additional support for this mechanism comes from our experiments at 16 and 80 K with N₂O, an efficient electron scavenger. Irradiated H₂O + N₂O ices always showed a peroxide band, as expected if N₂O protects H₂O₂ from destruction at the higher temperature. Clearly additional experiments are needed, perhaps with H₂¹⁸O or with other electron scavengers such as SF₆.

In conclusion, our work demonstrates that H₂O₂ is not produced in proton-irradiated H₂O ice at 80 K in sufficient abundance for IR detection. However, we have also shown that adding O₂ or CO₂ to the ice will raise the abundance of H₂O₂ to where it can be observed in the infrared. Our results suggest that the presence of O₂ in H₂O ice will produce detectable concentrations of H₂O₂ for the radiation environment of Europa discussed by Carlson *et al.* (1999). If, however, CO₂ is an important ice component on Europa, then adjustments to some of the modeled parameters will be required. Since Ganymede and Callisto receive only 7 and 0.2%, respectively, of the energy flux received by Europa, the steady-state concentrations of H₂O₂ on those satellites will be correspondingly lower than on Europa, placing the

¹ H atoms may react with H₂O₂ in a reaction similar to (4).

H_2O_2 IR band's intensity below the level of detection. (This assumes that the same models and ice mixtures apply to Ganymede and Callisto as to Europa). Finally we note that our results are based on proton radiolysis, protons being a major component of the jovian radiation environment. This environment also includes e^- , S^{n+} , and O^{n+} , and additional experiments will be required to understand the role of each species in forming H_2O_2 .

ACKNOWLEDGMENTS

The authors gratefully acknowledge R. W. Carlson for sending us a preprint describing the detection of H_2O_2 on Europa and for a copy of the NIMS IR data. We also benefited greatly from numerous discussions with R. E. Johnson. We thank J. F. Cooper for a preprint analyzing the plasma energy flux incident on the Galilean satellites. We acknowledge the cooperation of Steve Brown and Claude Smith of Goddard's Radiation Facility who operated the Van de Graaff accelerator. This research is supported by NASA through RTOPs 344-33-01 and 344-02-57.

REFERENCES

- Bonet-Maury, P. 1941. Photo-colorimétrique absolu. *C. R. Acad. Sci. Paris Biol.* **135**, 197–201.
- Bonet-Maury, P. 1944. Titrage photocalorimétrique de faibles quantités d'eau. *C. R. Acad. Sci. Paris* **218**, 117–119.
- Bonet-Maury, P., and M. Frilley 1944. La production d'eau oxygénée dans l'eau irradiée par les rayons X. *C. R. Acad. Sci. Paris* **218**, 400–402.
- Bonet-Maury, P., and M. Lefort 1948. Formation of hydrogen peroxide in water irradiated with X- and alpha-rays. *Nature* **162**, 381–382.
- Brewer, L., and J. L. Wang 1972. Infrared absorption spectra of isotopic ozone isolated in rare-gas matrices. *J. Chem. Phys.* **56**, 759–762.
- Carlson, R. W., M. S. Anderson, R. E. Johnson, W. D. Smythe, A. R. Hendrix, C. A. Barth, L. A. Soderblom, G. B. Hansen, T. B. McCord, J. B. Dalton, R. N. Clark, J. H. Shirley, A. C. Ocampo, and D. L. Matson 1999. Hydrogen peroxide on the surface of Europa. *Science* **283**, 2062–2064.
- Carlson, R. W., W. D. Smythe, K. Baines, E. Barbinis, K. Becker, R. Burns, S. Calcutt, W. Calvin, R. Clark, G. Danielson, A. Davies, P. Drossart, T. Encrenaz, F. Fanale, J. Granahan, G. Hansen, P. Herrera, C. Hibbitts, J. Hui, P. Irwin, T. Johnson, L. Kamp, H. Kieffer, F. Leader, E. Lellouch, R. Lopes-Gautier, D. Matson, T. McCord, R. Mehlman, A. Ocampo, G. Orton, M. Roos-Serote, M. Segura, J. Shirley, L. Soderblom, A. Stevenson, F. Taylor, J. Torson, A. Weir, and P. Weissman 1996. Near-infrared spectroscopy and spectral mapping of Jupiter and the Galilean satellites: Results from Galileo's initial orbit. *Science* **274**, 385–388.
- Cooper, J. F., R. E. Johnson, B. H. Mauk, H. B. Garrett, and N. Gehrels 2000. Energetic ion and electron irradiation of the icy Galilean satellites. *Icarus*, submitted.
- Gerakines, P. A., W. A. Schutte, and P. Ehrenfreund 1996. Ultraviolet processing of interstellar ice analogs. *Astron. Astrophys.* **312**, 289–305.
- Ghormley, J. A. 1967. Adsorption and occlusion of gases by the low-temperature forms of ice. *J. Chem. Phys.* **46**, 1321–1325.
- Ghormley, J. A., and A. C. Stewart 1956. Effects of γ -radiation on ice. *J. Am. Chem. Soc.* **78**, 2934–2939.
- Hall, D. T., P. D. Feldman, M. A. McGrath, and D. E. Strobel 1998. The far-ultraviolet oxygen airglow of Europa and Ganymede. *Astrophys. J.* **499**, 475–481.
- Hanel, R., B. Conrath, M. Flasar, L. Herath, V. Kunde, P. Lowman, W. Maguire, J. Pearl, J. Pirraglia, R. Samuelson, D. Gautier, P. Gierasch, L. Horn, S. Kumar, and C. Ponnampemra 1979. Infrared observations of the jovian system from Voyager 2. *Science* **206**, 952–956.
- Hudgins, D. M., S. A. Sandford, L. J. Allamandola, and A. G. G. M. Tielens 1993. Mid- and far-infrared spectroscopy of ices: Optical constants and integrated absorbances. *Astrophys. J. Suppl. Ser.* **86**, 713–870.
- Hudson, R. L., and M. H. Moore 1999. Laboratory studies of the formation of methanol and other organic molecules by carbon monoxide radiolysis: Relevance to comets, icy satellites, and interstellar ices. *Icarus* **140**, 451–461.
- Hudson, R. L., and M. H. Moore 1995. Far-IR spectral changes accompanying proton irradiation of solids of astrochemical interest. *Radiat. Phys. Chem.* **45**, 779–789.
- Lane, A. L., R. M. Nelson, and D. L. Matson 1981. Evidence for sulfur implantation in Europa's UV absorption band. *Nature* **292**, 38–39.
- Lannon, J. A., F. D. Verderame, and R. W. Anderson, Jr. 1971. Infrared spectrum of solid and matrix-isolated H_2O_2 and D_2O_2 . *J. Chem. Phys.* **54**, 2212–2223.
- Lefort, M. 1955. Chimie des radiations des solutions aqueuses. Aspects actuels des résultats expérimentaux. In *Actions Chimiques et Biologiques des Radiations* (M. Haissinsky, Ed.), Vol. 1, pp. 93–204. Masson, Paris.
- McCord, T. B., R. W. Carlson, W. D. Smythe, G. B. Hansen, R. N. Clark, C. A. Hibbitts, F. P. Fanale, J. C. Granahan, M. Segura, D. L. Matson, T. V. Johnson, and P. D. Martin 1997. Organics and other molecules in the surfaces of Callisto and Ganymede. *Science* **278**, 271–275.
- McCord, T. B., G. B. Hansen, R. N. Clark, P. D. Martin, C. A. Hibbitts, F. P. Fanale, J. C. Granahan, M. Segura, D. L. Matson, T. V. Johnson, R. W. Carlson, W. D. Smythe, G. E. Danielson, and the NIMS Team 1998. Non-water ice constituents in the surface material of the icy Galilean satellites from the Galileo near-infrared mapping spectrometer investigation. *J. Geophys. Res.* **103**, 8603–8626.
- Moore, M. H., and R. L. Hudson 1998. Infrared study of ion-irradiated water-ice mixtures with organics relevant to comets. *Icarus* **135**, 518–527.
- Moore, M. H., and R. L. Hudson 1992. Far-infrared spectral studies of phase changes in water ice induced by proton irradiation. *Astrophys. J.* **401**, 353–360.
- Moore, M. H., R. F. Ferrante, and J. A. Nuth, III 1996. Infrared spectra of proton-irradiated ices containing methanol. *Planet. Space Sci.* **44**, 927–935.
- Noll, K. S., R. Johnson, A. L. Lane, D. Cruikshank, Y. Pendleton, T. Roush, D. Domingue, and H. Weaver 1995. Ion-induced chemistry on icy satellite surfaces: Evidence from Hubble Space Telescope ultraviolet spectra. *Am. Astron. Soc.* **187**, 4217N.
- Noll, K. S., R. E. Johnson, A. L. Lane, D. L. Domingue, and H. A. Weaver 1996. Detection of ozone on Ganymede. *Science* **273**, 341–343.
- Noll, K. S., R. E. Johnson, M. A. McGrath, and J. J. Caldwell 1997. Detection of SO_2 on Callisto with the Hubble Space Telescope. *J. Geophys. Res. Lett.* **24**, 1139–1142.
- Orton, G. S., J. R. Spencer, L. D. Travis, T. Z. Martin, and L. K. Tamppari 1996. Galileo photopolarimeter-radiometer observations of Jupiter and the Galilean satellites. *Science* **274**, 389–391.
- Pettersson, M., S. Tuominen, and M. Räsänen 1997. IR spectroscopic study of H_2O_2 , HDO_2 and D_2O_2 isolated in Ar, Kr, and Xe matrices. *J. Phys. Chem. A* **101**, 1166–1171.
- Smythe, W. D., R. W. Carlson, A. Ocampo, D. L. Matson, and T. B. McCord 1998. Galileo NIMS measurements of the absorption bands at 4.03 and 4.25 microns in distant observations of Europa. *Bull. Am. Astron. Soc.* **30**, 5507.
- Spencer, J. R., W. M. Calvin, and M. J. Person 1995. CCD spectra of the Galilean satellites: Molecular oxygen on Ganymede. *J. Geophys. Res.* **100**, 19049–19056.
- Swallow, A. J. 1973. *Radiation Chemistry, an Introduction*. Wiley, New York.